Journal of Non-Crystalline Solids 385 (2014) 163–168

Contents lists available at ScienceDirect

Journal of Non-Crystalline Solids

journal homepage: www.elsevier.com/ locate/ jnoncrysol

Tunable full-color emitting borosilicate glasses via utilization of Ce^{3+} ions as multiple energy transfer contributors

Tian-Shuai Lv [a], Xu-Hui Xu [a,b], Xue Yu [a,b], Hong-Ling Yu [a], Da-Jian Wang [c], Da-Cheng Zhou [a,b], Jian-Bei Qiu [a,b,*]

[a] School of Materials Science and Engineering, Kunming University of Science and Technology, Xuefu Rd, Kunming 650093, PR China
[b] Key Lab of Advanced Materials in Rare & Precious and Nonferrous Metals, Kunming University of Science and Technology, Ministry of Education, Xuefu Rd, Kunming 650093, PR China
[c] Institute of Materials Physics, Tianjin University of Technology, Tianjin 300384, PR China

ARTICLE INFO

Article history:
Received 21 September 2013
Received in revised form 14 November 2013
Available online 6 December 2013

Keywords:
Rare earth;
Ce^{3+};
Activators;
Energy transfer;
Borosilicate glasses

ABSTRACT

A series of trichromatic/white-emitting $15CaO–55B_2O_3–30SiO_2$ glasses co-doped with $Ce^{3+}/Tb^{3+}/Mn^{2+}$ were synthesized in air by a melt-quenching method. Ce^{3+} ions played a role as sensitizers in improving the photoluminescence performance of multi-activators. Dual energy transfer (ET) processes of $Ce^{3+} \rightarrow Tb^{3+}$ and $Ce^{3+} \rightarrow Mn^{2+}$ were observed in Ce^{3+}–Mn^{2+}–Tb^{3+} co-activated glasses. The hues of the fabricated glasses covered the regions from blue, green, to orange–red, and a wide-range-tunable warm white light emission was realized by tuning the ET proportion from excitation source to the co-activated Mn^{2+} and Tb^{3+} ions through utilizing Ce^{3+} ions as the multi-sensitizers. It indicates that these glasses are expected to be potential phosphor candidates for deep UV-pumped white-LED.

1. Introduction

As an important solid state lighting technology, white light-emitting diodes (W-LEDs) are promptly appearing in daily life due to characteristic merits such as in energy savings, compactness, and environmental friendliness [1–5]. They also have a wide range of fascinating applications in general illumination, backlit automobile lamps, devices indicators, and backlights for liquid-crystal displays [6]. The commercial available strategy to produce white-LED is combining a blue emission diode chip with a yellow-emitting $(Y,Gd)_3(Al,Ga)_5O_{12}:Ce^{3+}$ phosphor. Although the route of white light realization is inexpensive, simple, and convenient with high brightness, it suffers the intrinsic defects such as poor white light stability, poor correlated color temperature (CCT) and chromatic aberration [7]. Besides, the emitting color is significantly influenced by the thickness of coating-printed phosphor layer and the injection current. As an alternative, combining tri-color phosphors with ultraviolet (UV) diode chips to produce white light is highly favored with the recent fast development of ultraviolet diodes. In this path, the efficiency of the device is relatively low because of the strong re-absorption of blue light by red and green-emitting phosphors [8,9]. Therefore, it is quite significant and emergent to develop versatile single-component white emitting phosphors with ultraviolet LED chips [5,8]. Although various kinds of single-phased phosphors are intensively developed worldwide, the sealing materials for these phosphors, such as organic resins, still have been limited to non-high power or long wavelength excitation light sources due to the degradation [10]. Therefore, the authors have emphasized that inorganic glass phosphors can be employed as sealant for deep UV LED or high intensity and shorter wavelength excitation white-LED [10–12]. Compared with conventional phosphors, rare earth (RE) ions doped glasses are promising candidates for use in deep UV-pumped white-LED owing to many excellent advantages such as epoxy resin-free, easy mass production, lower production cost and higher irradiation resistance [13–16]. Recently, the primary work is mostly focused on borate and phosphate glasses. The weak mechanical capability as well as the low chemical stability has limited their further application. Note that $CaO–B_2O_3–SiO_2$ glasses are appropriate hosts to develop high efficient white light devices due to good solubility for RE ions, excellent optical properties, easy formation of any shape, and better physical and chemical performances [8,9].

Ce^{3+} ion exhibits excellent UV absorption coefficient due to its parity allowed 4f → 5d electric dipole transition. It gives emission band from ultraviolet to orange–red region in different hosts owing to the sensitivity of 5d energy level to outer environment which suggests that the emission band of Ce^{3+} can be tailored by adjusting glass components [17–19]. The emission band of Ce^{3+} has been widely observed in broad region from blue, green, and to yellow–orange for chalcohalide glasses, blue region for silicate glasses, near ultraviolet region for borate glasses and ultraviolet region for phosphate glasses [18,20–22]. The absorption cross sections of most RE ions are in the ultraviolet/near-ultraviolet region where the emission band of Ce^{3+} ions could cover via tuning the components of borosilicate glasses in the $CaO–B_2O_3–SiO_2$ system. Moreover, tunable emissions have been realized by co-doping multi-activators such as Ce^{3+}/Eu^{2+} [6], Ce^{3+}/Mn^{2+} [17,19], Eu^{2+}/Mn^{2+} [7,23], Sb^{3+}/Mn^{2+} [8] and Cu^{+}/Sm^{3+} [9] in proper materials. However, there is no report on Ce^{3+}–Tb^{3+}–Mn^{2+} co-doped

* Corresponding author. Tel.: +86 871 6518 8856; fax: +86 871 6533 4185.
E-mail address: qiu@kmust.edu.cn (J.-B. Qiu).

0022-3093/$ – see front matter © 2013 Elsevier B.V. All rights reserved.
http://dx.doi.org/10.1016/j.jnoncrysol.2013.11.025

glasses prepared under air condition to generate wide-range-tunable light emissions.

In this manuscript, we reported our recent results on realizing the full color tunable emissions in $15CaO–55B_2O_3–30SiO_2$ glasses using Ce^{3+} ions as the multi-sensitizers, which were synthesized in air atmosphere. ET processes of $Ce^{3+} \rightarrow Tb^{3+}$ and $Ce^{3+} \rightarrow Mn^{2+}$ have been investigated in detail. A wide-chromaticity-tunable photoluminescence in Mn^{2+}–Ce^{3+}–Tb^{3+} co-doped glasses was obtained via controlling the ET transferring proportion of $Ce^{3+} \rightarrow Mn^{2+}$ to $Ce^{3+} \rightarrow Tb^{3+}$. Our results indicate the potential applications of these glasses in the fabrication of white-LEDs.

2. Experimental

The host (in mol%) of borosilicate glasses has the constitution of $15CaO–55B_2O_3–30SiO_2$ (CBS). Glasses of 8 g batch of the composition of CBS: xCe^{3+}, yTb^{3+}, zMn^{2+} glasses were prepared by a melt-quenching method using high purity of B_2O_3, $MnCO_3$, SiO_2, $CaCO_3$, CeO_2, and TbF_3 as the raw chemicals. Then the samples were melted in corundum crucibles at 1500 °C in air for 1 h. After this synthesis, the crucibles were removed from the furnace, and the melts were poured onto a 400 °C stainless steel mold and then annealed at 550 °C for 4 h.

The glasses were polished to a thickness of 4 mm and cut to optical quality before subjecting them to optical characterization. The optical absorption spectra (ABS) of different glass examples were recorded on a HITACHI U-4100 type spectrophotometer. Photoluminescence spectra were measured by a HITACHI F-7000 fluorescent spectrophotometer with a 150 W Xe lamp as the static excitation source. The photoluminescence decay lifetime was performed on a Jobin Yvon FL3 fluorescence spectrophotometer. The color rendering index (CRI) of Ce^{3+}–Tb^{3+}–Mn^{2+} co-doped example was measured by using UV–Vis-near IR spectrophotocolorimeter (Everfine PMS-50, China). All measurements were carried out under room temperature.

3. Results and discussion

The UV–visible (UV–VIS) absorption spectra of typical glass samples are depicted in Fig. 1. The inset displays the enlarged absorption spectra around 410 nm. The host shows a single wide intense band at near 283 nm, which is ascribed to its inherent absorption, and it is found that the UV cut-off wavelength changed after Tb^{3+}, Ce^{3+} and Mn^{2+} introduction. In addition, the inset suggests that Mn^{2+} characteristic absorption bands which peaked at 410 nm are observed for CBS: $2.0Mn^{2+}$ and CBS: $0.04Ce^{3+}$,$0.4Tb^{3+}$,$2.0Mn^{2+}$ corresponding to $^6A_1(S) \rightarrow [^4A_1(G), {}^4E(G)]$ transitions of Mn^{2+} ions [8]. Moreover, the host and the sample which co-activated with Mn^{2+}, Tb^{3+} and Ce^{3+} demonstrate strong absorbability in UV region and high transmittance due to low absorbency in VIS region.

The photoluminescence emission (PL) spectra and excitation (PLE) spectra of Ce^{3+} singly doped CBS are illustrated in Fig. 2a. For Ce-doped glass, there is a coexistence of Ce^{3+} and Ce^{4+} in CBS prepared in air. Ce^{4+} shows no emission because of its closed shell electronic structures. Ce^{3+} ion gives wide emission band extending from the deep ultraviolet to visible region. In this regard, all Ce-doped specimens can be regarded as if only Ce^{3+} is present in glasses. CBS: $0.04Ce^{3+}$ glass sample demonstrates an asymmetric broad excitation band ($\lambda_{em} = 392$ nm) from 250 nm to 370 nm corresponding to two strong sub-bands centered at 302 nm and 320 nm that can be ascribed to different transitions from 4f ground state to crystal field-splitting 5d states of Ce^{3+} in glass. Furthermore, when excited by 319 nm, a wide asymmetrical blue band in the region from 345 to 510 nm in emission spectra with a maximum at about 392 nm is observed for the parity allowed electronic transitions from the lowest component of the excited 5d states to $^2F_{7/2}$ and $^2F_{5/2}$ energy levels of Ce^{3+} ions. The asymmetric blue emission band consists of two de-convoluted Gaussian profiles that peaked at 391 nm and 412 nm corresponding to an energy difference of about 1320 cm^{-1}. Compared with the well-known theoretical energy difference between $^2F_{7/2}$ and $^2F_{5/2}$ levels of Ce^{3+} ion (~2000 cm^{-1}), there is a deviation which should be contributed to the crystal-field splitting of the ground state of Ce^{3+} in glass. More importantly, it demonstrates that the PLE spectrum of CBS: $0.04Ce^{3+}$ from 200 nm to 400 nm is well consistent with the emission of the deep UV LED chip, suggesting the potential application in deep UV white-LED.

The PLE and PL spectra of Mn^{2+} singly doped glass is shown in Fig. 2b. For CBS: $1.0Mn^{2+}$, it is difficult to pump the excitation transitions of Mn^{2+} due to its forbidden d → d transition. It exhibits a very weak orange–red band emission at 601 nm under its characteristic excitation of 410 nm, which is assigned to the spin-forbidden $^4T_1(G)$-$^6A_1(S)$ transition of Mn^{2+} with its PLE bands at about 357 and 410 nm, corresponding to the transitions from $^6A_1(S)$ to $^4T_2(D)$ and $^4E(G, {}^4A_1(G))$ levels of Mn^{2+}, respectively. Comparing the PL spectrum of CBS: $0.04Ce^{3+}$ with the PLE spectrum of CBS: $1.0Mn^{2+}$, a strong spectral overlap between the broad emission band of Ce^{3+} and excitation transitions of Mn^{2+} in the range of 365–510 nm is observed. Accordingly, an efficient ET process from $Ce^{3+} \rightarrow Mn^{2+}$ is expected, which demonstrates that the emission intensity of Mn^{2+} can be considerably

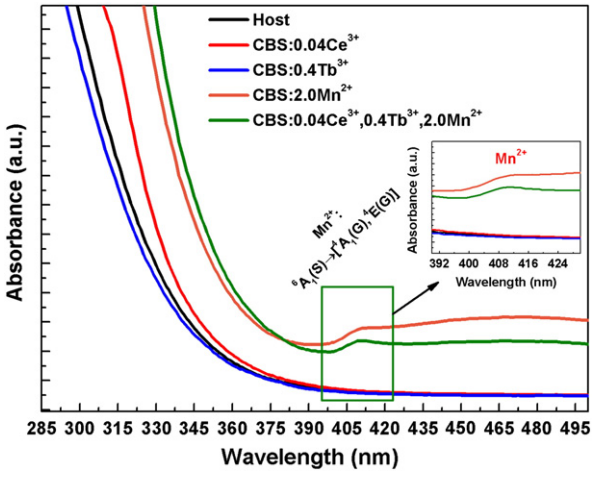

Fig. 1. The UV–VIS absorption spectra of the host, CBS: $0.04Ce^{3+}$, CBS: $0.4Tb^{3+}$, CBS: $2.0Mn^{2+}$ and CBS: $0.04Ce^{3+}$, $0.4Tb^{3+}$, $2.0Mn^{2+}$ borosilicate glasses.

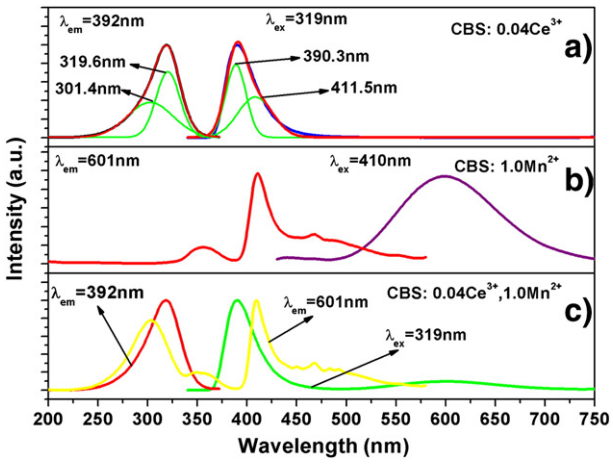

Fig. 2. Typical PLE and PL spectra of CBS: $0.04Ce^{3+}$ (a), CBS: $1.0Mn^{2+}$ (b), and CBS: $0.04Ce^{3+}$, $1.0Mn^{2+}$ (c) glasses.

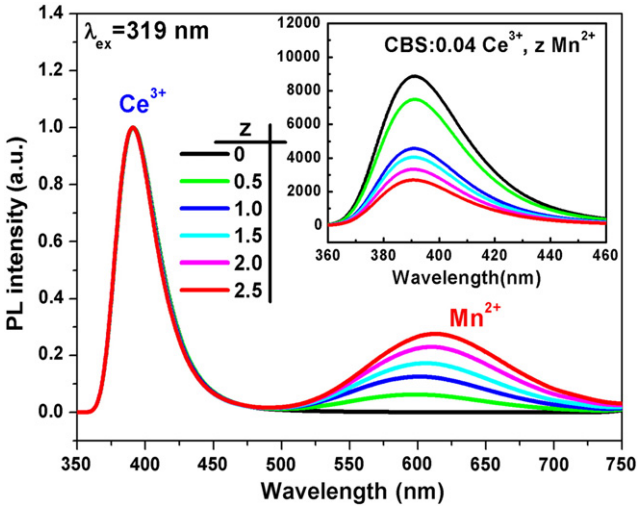

Fig. 3. PL spectra for CBS: $0.04Ce^{3+}$, zMn^{2+} (z = 0, 0.5, 1.0, 1.5, 2.0 and 2.5) excited by 319 nm. The inset shows the Ce^{3+} emission bands.

enhanced via introducing Ce^{3+} as a sensitizer. Fig. 2c gives the PL and PLE spectra of CBS: $0.04Ce^{3+}$, $1.0Mn^{2+}$. It is clearly seen in the range of 200–370 nm that the excitation spectrum monitoring at 601 nm of Mn^{2+} is similar to that of monitoring at purple–blue emission (392 nm) of Ce^{3+}, further indicating the occurrence of ET from Ce^{3+} to Mn^{2+} in Ce^{3+}–Mn^{2+} co-doped glass.

For the further evidence of ET from $Ce^{3+} \rightarrow Mn^{2+}$, the concentration dependence of the PL spectra of CBS: $0.04Ce^{3+}$, zMn^{2+} (z = 0, 0.5, 1.0, 1.5, 2.0 and 2.5) is depicted in Fig. 3. Under the characteristic excitation wavelength of 319 nm for Ce^{3+}, both the purple–blue band from Ce^{3+} and the orange–red luminescence from Mn^{2+} are observed. With increasing Mn^{2+} content from z = 0 to 2.5, the relative emission intensity of Ce^{3+} decreases systemically, whereas that of the PL intensity of Mn^{2+} increases at first with increasing z when z is <2.0, and then decreases which is ascribed to the concentration quenching of Mn^{2+}–Mn^{2+}. Under the 319 nm excitation, no emission from Mn^{2+} is observed for Mn^{2+} singly doped sample. All results above demonstrate that the high light output of Mn^{2+} is actually originated from the ET process from $Ce^{3+} \rightarrow Mn^{2+}$ using Ce^{3+} ions as the efficient sensitizers. Furthermore, the whole ET efficiency (η_T) from sensitizer-Ce^{3+} → activator-Mn^{2+} ions in the CBS: $0.04Ce^{3+}$, zMn^{2+} glass system can be estimated using the formula [9,17]

$$\eta_T = 1 - \frac{I_S}{I_{S0}} \quad (1)$$

where η_T is the ET efficiency and I_S and I_{S0} are the emission intensities of a sensitizer (Ce^{3+}) in the presence and absence of an activator (Mn^{2+}/Tb^{3+}), respectively.

Fig. 4a illustrates the results of ET efficiency from Ce^{3+} to Mn^{2+}, under a UV excitation of 319 nm. The η_T value of CBS: $0.04Ce^{3+}$, zMn^{2+} could be derived as a function of z and gradually increases with increasing Mn^{2+}-activating content, in which the maximal ET efficiency can reach about 70% when z = 2.5. It can be clearly observed that the increscent rate of the η_T gradually decreases with the increasing Mn^{2+}. This result indicates that the ET efficiency from $Ce^{3+} \rightarrow Mn^{2+}$ will gradually trend to saturation with a continuous supplement of Mn^{2+}-doping content.

Based on the ET from Ce^{3+} to Mn^{2+} analyzed above, tunable hues are obtained. The CIE chromaticity diagram for CBS: $0.04Ce^{3+}$, zMn^{2+} is calculated at different z values, as shown in Fig. 4b. With increasing Mn^{2+} content, the CIE coordinates change systematically among (0.17, 0.03), (0.30, 0.19), (0.37, 0.27), (0.40, 0.30), (0.43, 0.31), and (0.45, 0.32), for z = 0, 0.5, 1.0, 1.5, 2.0, and 2.5, corresponding to the tunable sample hues that varies gradually from purplish-blue to purplish-pink (near white region) and eventually to yellowish-orange region.

As analyzed above, it is found that the orange–red luminescence of Mn^{2+} can be enhanced through ET process from $Ce^{3+} \rightarrow Mn^{2+}$. However, another pivotal issue is the lack of green components depending on the RGB (red, green and blue light emission) mechanism to generate warm white-light emission. Thus, a strategy has been put forward to improve luminescence performance of Tb^{3+} by introducing Ce^{3+} ion as a sensitizer for Tb^{3+} in Ce^{3+}–Mn^{2+}–Tb^{3+} co-activated glasses. Hence, the Ce^{3+}/Tb^{3+} doped glasses have been studied firstly to obtain a better understanding of interaction between Tb^{3+} and Ce^{3+} ions.

The PLE/PL spectra of Ce^{3+}/Tb^{3+} singly doped glasses are presented in Fig. 5a and b, respectively. As shown in Fig. 5b, there are several weak emission bands located at 623 nm, 589 nm and 545 nm, which are ascribed to the $^5D_4 \rightarrow {}^7F_J$ (J = 3, 4 and 5) multiple transitions of Tb^{3+},

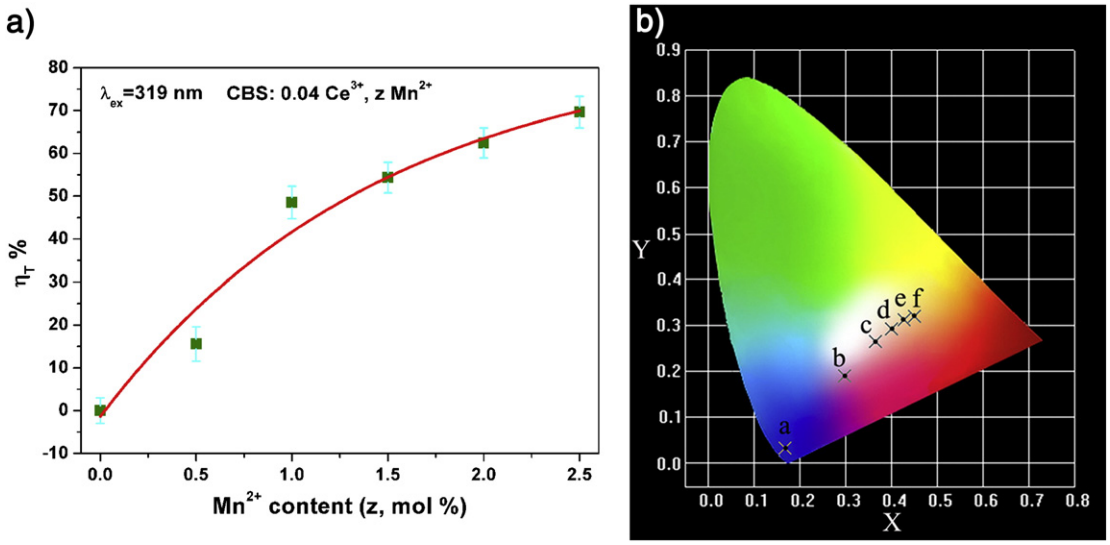

Fig. 4. (a) ET efficiency (η_T) from Ce^{3+} to Mn^{2+} in Ce^{3+}–Mn^{2+} co-doped glasses. (b) Evolution of CIE 1931 chromaticity coordinates (X, Y) for CBS: $0.04Ce^{3+}$, zMn^{2+} (z = 0–2.5) from (a) to (f) with the increase of Mn^{2+} content.

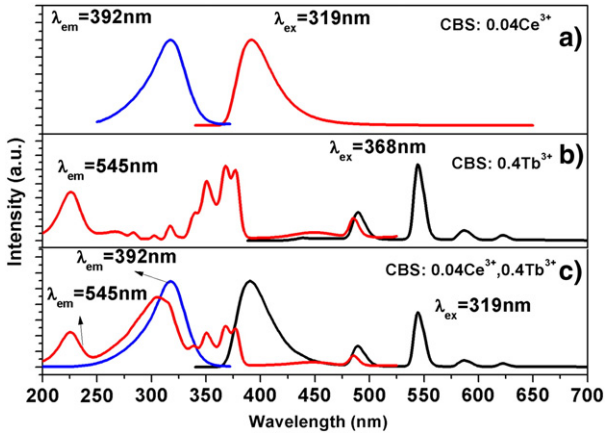

Fig. 5. The PL spectra and PLE spectra of RE ions doped glasses: (a) CBS: $0.04Ce^{3+}$, (b) CBS: $0.4Tb^{3+}$, (c) CBS: $0.04Ce^{3+}$, $0.4Tb^{3+}$.

respectively. For the excitation spectrum of CBS: $0.4Tb^{3+}$, it shows that there is a broad excitation band centered at about 226 nm due to spin-allowed 4f–5d transitions of Tb^{3+}, and several absorption bands at about 300–400 nm ascribed to the forbidden f–f transitions of Tb^{3+} ions. Compared with the PL spectrum of CBS: $0.04Ce^{3+}$ (Fig. 5a), CBS: $0.4Tb^{3+}$ exhibits very weak green fluorescence originated from $^5D_4$ emission of Tb^{3+}, under its characteristic excitation of 368 nm. It indicates that Tb^{3+} could not be efficiently activated by UV-wavelength radiation in this Tb^{3+}-singly doped glass.

It is found that there is a significant spectral overlap between the PL spectrum of Ce^{3+} and the PLE spectrum of Tb^{3+} which indicates the probability of ET from Ce^{3+} to Tb^{3+}. An intense green emission of Tb^{3+} may be obtained through ET process of $Ce^{3+} \rightarrow Tb^{3+}$ according to Dexter's theory [13,24]. Fig. 5c presents the PL and PLE spectra of Tb^{3+}–Ce^{3+} co-activated CBS: $0.04Ce^{3+}$, $0.4Tb^{3+}$ glass sample. Under the 319 nm excitation, CBS: $0.04Ce^{3+}$, $0.4Tb^{3+}$ exhibits a broad blue emission from Ce^{3+}, as well as a narrow yellowish-green band emission from Tb^{3+}. When the characteristic emission of Tb^{3+} ($\lambda_{em} = 545$ nm) is monitored, the excitation spectrum not only contains the typical excitation band of Tb^{3+}, but also includes a broad additional excitation band at about 250–350 nm from Ce^{3+}, demonstrating the existence of ET from $Ce^{3+} \rightarrow Tb^{3+}$. Upon the 319 nm excitation, almost no fluorescence has been observed in Tb^{3+} singly-doped glass or the host. These results suggest that the enhancement emission of Tb^{3+} is attributed to the occurrence of ET from Ce^{3+} to Tb^{3+} in Ce^{3+}–Tb^{3+}-codoped glass.

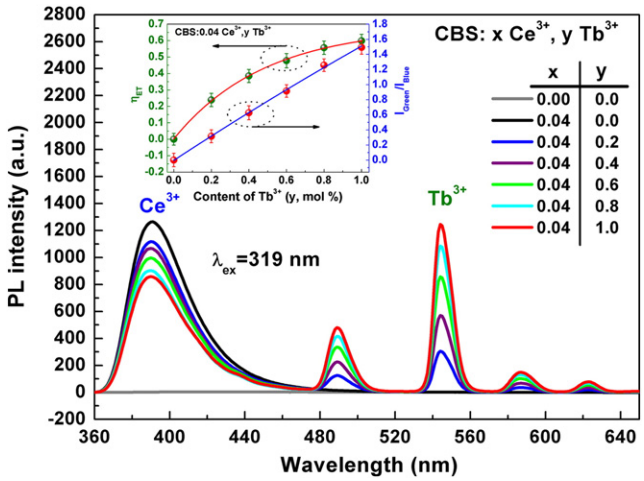

Fig. 6. Emission spectra ($\lambda_{ex} = 319$ nm) of glass host, Ce^{3+}–Tb^{3+} co-activated CBS. The inset shows energy transfer efficiency (η_{ET}) of CBS: Ce–Tb system.

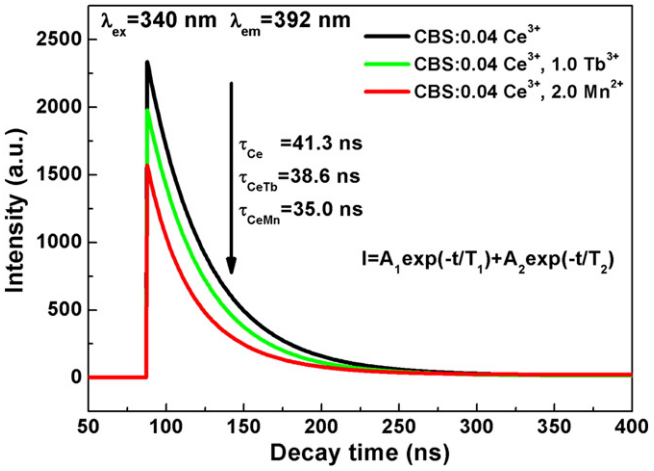

Fig. 7. Representative fluorescence lifetimes (τ) of Ce^{3+} emission at 392 nm in CBS: $0.04Ce^{3+}$, CBS: $0.04Ce^{3+}$, $1.0Tb^{3+}$ and CBS: $0.04Ce^{3+}$, $2.0Mn^{2+}$ under 340 nm excitation.

To further confirm the occurrence of ET from Ce^{3+} to Tb^{3+}, a series of PL spectra ($\lambda_{ex} = 319$ nm) for CBS: $0.04Ce^{3+}$, yTb^{3+} ($y = 0, 0.2, 0.4, 0.6, 0.8, 1.0$) have been carried out as presented in Fig. 6. With increasing Tb^{3+} concentration, the emission intensity of Ce^{3+} ion decreased monotonically, whereas that of Tb^{3+} increased simultaneously, which supports the existence of energy transfer from Ce^{3+} to Tb^{3+}. And the ET efficiency (η_T) of $Ce^{3+} \rightarrow Tb^{3+}$ can be estimated according to Eq. (1). The η_T value of Ce^{3+}–Tb^{3+} co-doped glass can be realized as a function of y and is shown in the inset of Fig. 6, in which the maximum ET efficiency has reached 59.24% when $y = 1.0$. All of the characteristics indicate that the Ce^{3+} ion, as a sensitizer, has efficaciously transferred the energy from excitation source to Tb^{3+} ions in glass.

To further validate the dual ET processes of $Ce^{3+} \rightarrow Tb^{3+}$ and $Ce^{3+} \rightarrow Mn^{2+}$, the decay curves of CBS: $0.04Ce^{3+}$, CBS: $0.04Ce^{3+}$, $1.0Tb^{3+}$ and CBS: $0.04Ce^{3+}$, $2.0Mn^{2+}$ excited at 340 nm and monitored at 392 nm are measured and depicted in Fig. 7. It is observed that the decay curves of Ce^{3+} fluorescence can be well fitted to a dual-exponential decay mode attributed to two distinct fluorescence centers in glass host [25–27]. And the curves can be expressed by the following formula with goodness fits [26,28]:

$$I = A_1 e^{-t/\tau_1} + A_2 e^{-t/\tau_2} \quad (2)$$

where I is the integrated fluorescence intensity of Ce^{3+}; A_1 and A_2 are constants; t is the fluorescence lifetime, and τ_1 and τ_2 stand for the rapid and slow luminescence lifetimes for the exponential

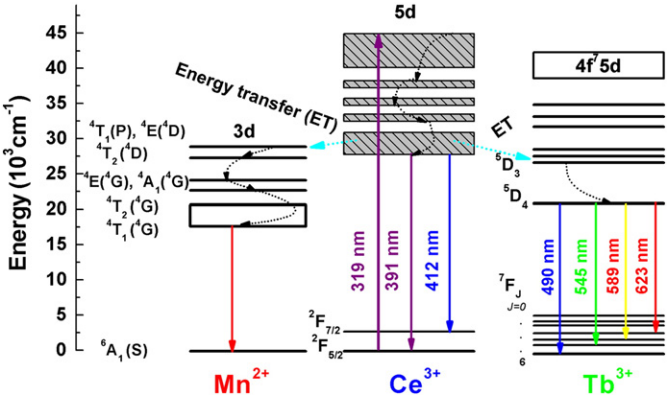

Fig. 8. Energy diagram of the ET mechanism for Ce^{3+}–Mn^{2+} and Ce^{3+}–Tb^{3+} pairs in Ce^{3+}–Mn^{2+}–Tb^{3+} co-doped glasses.

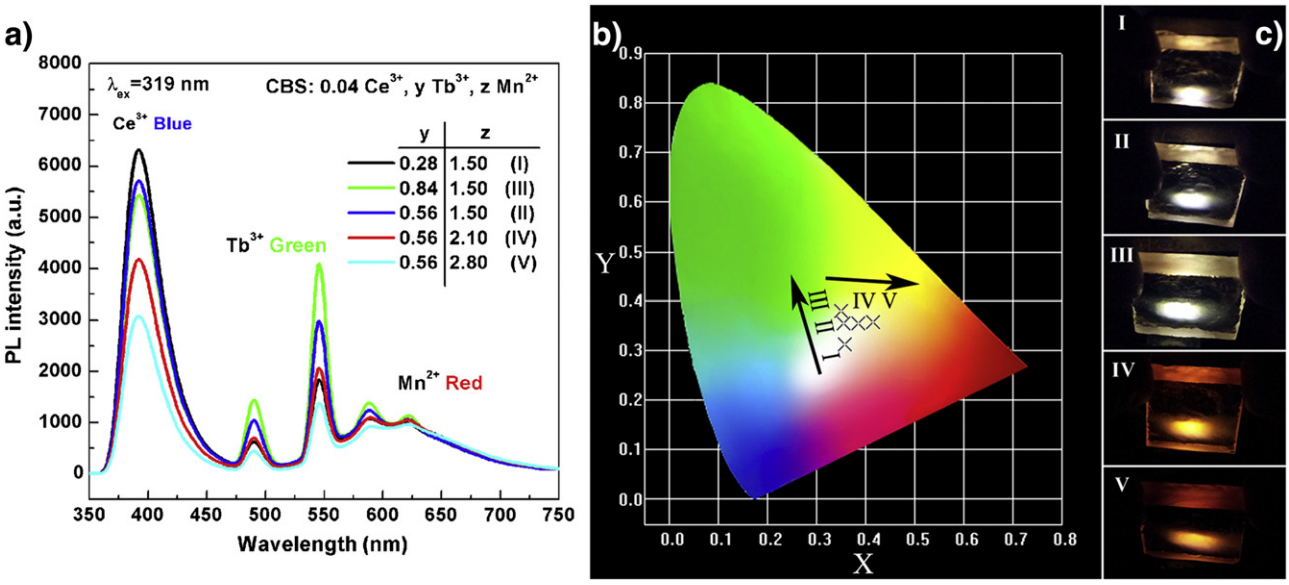

Fig. 9. (a) PL spectra (λ_{ex} = 319 nm) of CBS: 0.04Ce^{3+}, yTb^{3+}, zMn^{2+} (y = 0.28, 0.56, 0.84; z = 1.5, 2.1, 2.8); the corresponding CIE coordinates (b) and photos (c).

compositions, respectively. With these parameters, the average photoluminescence lifetimes for Ce^{3+} in glass can be resolved and calculated by the equation as follows:

$$\tau^* = \frac{A_1\tau_1^2 + A_2\tau_2^2}{A_1\tau_1 + A_2\tau_2}. \quad (3)$$

The average decay lifetimes of Ce^{3+} emission are calculated to be about 41.3 ns, 38.6 ns, and 35.0 ns for τ_{Ce}, τ_{CeTb} and τ_{CeMn}, respectively. The increase of Tb^{3+} and Mn^{2+} doping contents leads to faster fluorescence decay of Ce^{3+} emission that can be assigned to the ET process from Ce^{3+} to neighboring Tb^{3+} and Mn^{2+} ions in glass. The result further strongly supports the dual ET processes from Ce^{3+} to Tb^{3+} and from Ce^{3+} to Mn^{2+}, utilizing Ce^{3+} ions as the multi-sensitizers, simultaneously.

For the doubt of the luminescence behavior of Ce^{3+} ions as multi-sensitizers, a corresponding scheme of Ce^{3+}–Mn^{2+}–Tb^{3+} energy levels is shown in Fig. 8. Upon 319 nm excitation, electrons are pumped to 5d level of Ce^{3+} and transfer to the lowest component of 5d through a non-radiation relaxation process. Due to the energy levels of lowest pumped 5d state of Ce^{3+} are almost equal to the energy levels of Tb^{3+} ($^5D_3$ and other levels), the ET process of $Ce^{3+} \rightarrow Tb^{3+}$ can be easily occurred. Consequently, a part of energy of Ce^{3+} transfers to the $^5D_3$ and lower levels of Tb^{3+} by non-radiation relaxation. Then, Tb^{3+} relaxes to $^5D_4$ levels from $^5D_3$ and other higher levels through an irradiation process. Finally, Tb^{3+} exhibits green emission due to the transitions of Tb^{3+}: $^5D_4$–^7F_J (J = 3–6) [15,28]. Likewise, excited 5d state of Ce^{3+} is energetically close to the ($^4T_1$(P), ^4E(^4D)) level and other levels of Mn^{2+}. Thus, these excited Ce^{3+} ions rapidly relax from excited state to ground states through an irradiation process and then efficiently transfer the energy to the neighboring activator-Mn^{2+} ions, stimulating Mn^{2+} from ground state ($^6A_1$) to the excited level (^4E(^4G), $^4A_1$(^4G)). Subsequently, the level (^4E(^4G), $^4A_1$(^4G)) populated Mn^{2+} ions experience a multi-phonon relaxation mechanism to energy level ($^4T_1$(^4G)) and radiatively relax to ground energy level ($^6A_1$) of Mn^{2+}, exhibiting characteristic orange–red emissions, ultimately [8].

It's worth noting that the ET from sensitizer to multi-activators is a facile approach to generate tunable white-light emission via regulating the tricolor light at an appropriate ratio. Our experimental results have notarized this situation. In our case, the CBS: 0.04Ce^{3+} exhibits bright blue emission owing to 5d → 4f transition of Ce^{3+}, and high efficient ET from Ce^{3+} to Tb^{3+} is validated, resulting in strong green emission bands of Tb^{3+} and a color-tunable emission in Tb^{3+}–Ce^{3+} co-doped glass. Moreover, color-tunable emission is also obtained in Mn^{2+}–Ce^{3+} co-doped glass through the ET from Ce^{3+} to Mn^{2+}. It is reasonable to easily modulate the white light emission by accurately adjusting the ratio of the ET efficiencies between $Ce^{3+} \rightarrow Tb^{3+}$ and $Ce^{3+} \rightarrow Mn^{2+}$ with a fixed sensitizer content of Ce^{3+} in glass.

To further obtain ideal warm white light emission, a series of PL spectra of CBS: xCe^{3+}, yTb^{3+}, zMn^{2+} have been carried out as shown in Fig. 9a. The corresponding CIE coordinates and photos are displayed in Fig. 9b and c, respectively. When fixed Mn^{2+} doping content is at 1.5 mol%, the colors of CBS: 0.04Ce^{3+}, yTb^{3+}, 1.5Mn^{2+} vary from white to yellowish green region with the enhancement of y values from 0.28 to 0.84, i.e. the enhancement of green component. While for fixed Tb^{3+} doping content at 0.56 mol%, the colors of CBS: 0.04Ce^{3+}, 0.56Tb^{3+}, zMn^{2+} shift from white to yellow–orange with the increase of z values from 1.50 to 2.8, namely, the increase of orange–red component. To further understand the emission properties of Ce^{3+}–Tb^{3+}–Mn^{2+} co-doped glasses, the CCT and CRI of CBS:0.04Ce^{3+},0.56Tb^{3+},1.50Mn^{2+} (Fig. 9) were measured and calculated to be 4380 K and 88.4, respectively.

4. Conclusions

A series of tunable full-color emitting 15CaO–55B_2O_3–30SiO_2 glasses were fabricated in air by a melt-quenching method. Ce^{3+} could be significantly served as a highly efficient multi-sensitizer for activators. There are dual ET processes of $Ce^{3+} \rightarrow Tb^{3+}$ and $Ce^{3+} \rightarrow Mn^{2+}$ in Ce^{3+}–Mn^{2+}–Tb^{3+} co-activated glasses. The emitting hues of investigated specimens can be tuned from blue to green region via ET from Ce^{3+} to Tb^{3+} and from blue to yellowish-orange region via ET from Ce^{3+} to Mn^{2+}, respectively. More significantly, a wide-range-accommodative warm white-light emission was achieved by appropriately tuning the ET efficiencies of $Ce^{3+} \rightarrow Tb^{3+}$ and $Ce^{3+} \rightarrow Mn^{2+}$. Our results indicate that these glasses provide an original platform to design and manufacture novel luminous materials for deep UV and high-power light source excitation white-LED.

Acknowledgments

This work is financially supported by a grant from the National Natural Science Foundation of China (NSFC 51272097; 61265004; 51002068), the Nature and Science Fund from Yunnan Province

Ministry of Education (No.2011C13211708) and the Fund of National Natural Science Foundation for Youths of Yunnan (Grant No. 2012FD009).

References

[1] W.B. Im, N. George, J. Kurzman, S. Brinkley, A. Mikhailovsky, J. Hu, B.F. Chmelka, S.P. DenBaars, R. Seshadri, Adv. Mater. 23 (2011) 2300–2305.
[2] D. Haranath, S. Mishra, S. Yadav, R.K. Sharma, L.M. Kandpal, N. Vijayan, M.K. Dalai, G. Sehgal, V. Shanker, Appl. Phys. Lett. 101 (2012)(221905-221905).
[3] C.J. Zhao, J.L. Cai, R.Y. Li, S.L. Tie, X. Wan, J.Y. Shen, J. Non-Cryst. Solids 358 (2012) 604–608.
[4] X.Y. Sun, S. Wu, X. Liu, P. Gao, S.M. Huang, J. Non-Cryst. Solids 368 (2013) 51–54.
[5] T. Tsuboi, J. Non-Cryst. Solids 356 (2010) 1919–1927.
[6] X.F. Song, R.L. Fu, S. Agathopoulos, H. He, X.R. Zhao, X.D. Yu, J. Am. Ceram. Soc. 94 (2011) 501–507.
[7] W.-R. Liu, C.-H. Huang, C.-W. Yeh, J.-C. Tsai, Y.-C. Chiu, Y.-T. Yeh, R.-S. Liu, Inorg. Chem. 51 (2012) 9636–9641.
[8] H. Guo, R.F. Wei, Y.L. Wei, X.Y. Liu, J.Y. Gao, C.G. Ma, Opt. Lett. 37 (2012) 4275–4277.
[9] R. Wei, C. Ma, Y. Wei, J. Gao, H. Guo, Opt. Express 20 (2012) 29743–29750.
[10] H. Masai, T. Tanimoto, T. Fujiwara, S. Matsumoto, Y. Tokuda, T. Yoko, Opt. Express 20 (2012) 27319–27326.
[11] K. Davitt, Y.-K. Song, W. Patterson Iii, A. Nurmikko, M. Gherasimova, J. Han, Y.-L. Pan, R. Chang, Opt. Express 13 (2005) 9548–9555.
[12] J. Edmond, A. Abare, M. Bergman, J. Bharathan, K. Lee Bunker, D. Emerson, K. Haberern, J. Ibbetson, M. Leung, P. Russel, D. Slater, J. Cryst. Growth 272 (2004) 242–250.
[13] L. Yang, N. Dai, Z. Liu, Z. Jiang, J. Peng, H. Li, J. Li, M. Yamashita, T. Akai, J. Mater. Chem. 21 (2011) 6274–6279.
[14] X.L. Liang, Y.X. Yang, S.F. Wang, G.R. Chen, J. Non-Cryst. Solids 357 (2011) 2255–2258.
[15] X. Wan, Y.Q. Lin, S.L. Tie, J.Y. Shen, J. Non-Cryst. Solids 357 (2011) 3424–3429.
[16] R. Ye, Z. Cui, Y. Hua, D. Deng, S. Zhao, C. Li, S. Xu, J. Non-Cryst. Solids 357 (2011) 2282–2285.
[17] C.-H. Huang, T.-W. Kuo, T.-M. Chen, ACS Appl. Mater. Interfaces 2 (2010) 1395–1399.
[18] M. Nikl, K. Nitsch, E. Mihokova, N. Solovieva, J.A. Mares, P. Fabeni, G.P. Pazzi, M. Martini, A. Vedda, S. Baccaro, Appl. Phys. Lett. 77 (2000) 2159–2161.
[19] Y. Liu, X. Zhang, Z. Hao, X. Wang, J. Zhang, Chem. Commun. 47 (2011) 10677–10679.
[20] W. Chewpraditkul, Y. Shen, D. Chen, B. Yu, P. Prusa, M. Nikl, A. Beitlerova, C. Wanarak, Opt. Mater. 34 (2012) 1762–1766.
[21] G.K. DasMohapatra, Mater. Lett. 35 (1998) 120–125.
[22] C. Shen, Q. Yan, Y. Xu, G. Yang, W. Shufen, X. Zhongwen, G. Chen, J. Am. Ceram. Soc. 93 (2010) 614–617.
[23] Q. Luo, X.S. Qiao, X.P. Fan, B. Fan, X.H. Zhang, J. Am. Ceram. Soc. 94 (2011) 1670–1674.
[24] D.L. Dexter, Phys. Rev. 108 (1957) 630–633.
[25] W.B. Im, S. Brinkley, J. Hu, A. Mikhailovsky, S.P. DenBaars, R. Seshadri, Chem. Mater. 22 (2010) 2842–2849.
[26] M. Shang, G. Li, X. Kang, D. Yang, D. Geng, J. Lin, ACS Appl. Mater. Interfaces 3 (2011) 2738–2746.
[27] S. Park, T. Vogt, J. Lumin. 129 (2009) 952–957.
[28] Y. Shi, G. Zhu, M. Mikami, Y. Shimomura, Y. Wang, Mater. Res. Bull. 48 (2013) 114–117.